Journal of Non-Oxide Glasses Vol. 12, No. 1, January - March 2020, p. 1 - 6

SYNTHESIS, CHARACTERIZATION AND OPTICAL BAND GAP OF CdO NANOFIBERS DERIVED FROM ANTHRANILIC ACID PRECURSORS VIA A THERMAL DECOMPOSITION ROUTE

AH Al-BAGAWI*
Chemistry Department, Faculty of Science, University of Ha'il, Hail, 1560, KSA

This study aims to synthesis Cadmium Oxide (CdO) nanofibers with low cost, by thermal decomposition route using anthranilic acid precursors. Characterized by ^{1}H-NMR spectrum, Infrared spectral analysis. Thermo gravimetric analysis (TGA) was applied to determine the thermal behavior of the precursors decompose leaving the oxide. The crystalline structures were investigated by X-ray diffraction (XRD), the morphology of particles by TEM.The average diameter of fiber around 6 nm -59 nm which supported by TEM image. The analysis of the optical absorption data revealed that the optical band gap Eg was direct transitions and support the desirable feature for the optoelectronic devices based on its band gap energy value.

(Received October 1, 2019; Accepted January 16, 2020)

Keywords: Cadmium Oxide, Nano Fiber, Metal complex

1. Introduction

This century has witnessed a wonderful escalation in the field of science and technology, for which the support of nanotechnology is much extensive. In the past decade, nanoscale research has opened new opportunities for a wide number of technological applications. Due to their special optical, magnetic, electrical, and catalytic properties and improved physical properties like mechanical hardness, thermal stability, or chemical passivity [1], metal oxide nanostructures are widely used as paint pigments, cosmetics, pharmaceuticals, medical diagnostics, catalysts and supports, membranes and filters, batteries and fuel cells, electronics, magnetic and optical devices, flat panel displays, biomaterials, structured materials, and protective coatings [2].

Nanostructures based on cadmium oxide is particularly interesting because of their n-type conductivity with a wide band gap (2.2 eV) which makes this material more suitable for modern technologies. CdO has promising applications in catalysts [3, 4], gas sensors [5, 6], solar cells [7, 8], paint pigments, and so on.

There are several accepted techniques for the preparation of CdO nanoparticles such as sol-gel method [9, 10], microemulsion method [11, 12], precipitation method, thermal decomposition [13], hydrothermal method [14, 15], chemical coprecipitation method [16], and thermal evaporation [17].

2. Experimental details

All the chemicals used were analytical reagents and were used as it is without further purification. Anthranilic acid was purchased from (Merck), while 4-aminophenol was purchased from (Sigma-Aldrich). $CdCl_2$. 2.5H2O were purchased from (BDH). Ethanol was purchased from CARLOERBA with purity 99.9 %, while Dimethylsulfoxide was purchased from (Sigma-Aldrich) with purity 99%.

2.1. Synthesis of the precursors

---

[*] Corresponding author: amalelbagawi@gmail.com

Three Ternary complex were synthesized by dissolving (0.01 mol) of both anthranilic acid and P-amino phenol in 100 ml distilled water, by slight heating and stirring until the solution becomes clear. Then, the calculated amount (0.01mol) in 50 ml distilled water of the metal chlorides ($CdCl_2.2.5H_2O$) was added to the clear solution of the two ligands. On addition, a precipitate has formed, filtrated off, washed with distilled water and then left at room temperature overnight.

2.2. Synthesis of Metal Oxides Nano particles

The as-prepared [Cd(Anth)(p-AmPh)2]1.5H2O complex were ignited in a muffle furnace at a rate of 50 C/MIN were ignited in a muffle furnace at 600 ^{o}C for 2 h in air. CdO nanoparticles were obtained

3. Results and discussion

3.1. IR spectra

The active sites which coordinate to the metal ions to form the ternary complexes were determined by careful comparison of the spectra of anthranilic acid, p-aminophenol and the metal complexes. The results were shown in Fig. 1 and tabulated in Table 1.

Table 1. IR spectra of Cd(II) complex result.

Compound	ν(OH)	$\nu_{as}(COO^-)$	δ NH_2)	$\nu_s(COO^-)$	δ(OH)	ν(Cd-O)	ν(Cd-N)
$[Cd(Anth)(p\text{-}mPh)_2]1.5H_2O$	33420	1619	1587, 1531	1328	1068	518	450

Anthranilic acid showed bands at 3324, 3239, 1630 and 1585 cm^{-1} attributed to ν_{as} NH_2, ν_s NH_2, ν_{as} COO^- and δNH_2, respectively [18].The spectrum of p-aminophenol shows bands at 3400, 3341 and 3282 cm^{-1} and 1535 cm^{-1} due to ν OH, ν_{as} NH_2, ν_s NH_2 and δNH_2, respectively [19].

The spectra of the complexes exhibit broad band centered around 3430 cm^{-1} due to the stretching vibrations of hydrogen bonded phenolic OH. The stretching vibrations of the asymmetric ν_{as} COO^- group of anthranilic acid has been shifted to the range 1612-1619 cm^{-1}. The shift was attributed to the bonding of this group to the metal ions. The symmetric stretching vibrations of the ν_s COO^- group appears in the range 1324-1328 cm^{-1}. The difference between the asymmetric and symmetric stretching vibrations indicates the monodentate nature of this group [20-24].

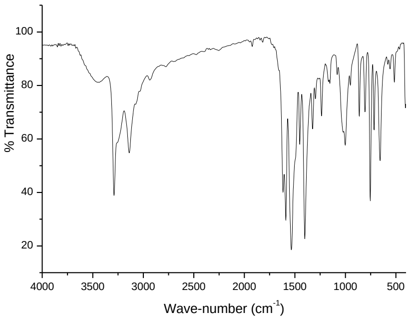

Fig. 1. IR spectra of Cd(II) complex.

The band due to δNH_2 of the anthranilic acid has been shifted to *ca.* 1592 cm^{-1} as a result of coordination of this group to the metal ions. The spectra show bands in the region 1068-1083 cm^{-1} due to δOH. In the complexes the band at 1530 of δNH_2 group of p-aminophenol remains more or less unaltered. From these observations it could be suggested that anthranilic acid coordinates to the metal ions as bidentate ligand through the carboxylate group in the deprotonated form and amino nitrogen. In the same time p- aminophenol coordinates to the metal ions in a monodentate mode through hydroxyl group. New bands appear in the range 515-518 and 435-450 cm^{-1} attributed to ν M-O and, ν M-N respectively [25-28]

3.2. 1H-NMR spectrum of Cd2+ complexes

The ^{1}H-NMR spectrum of Cd(II) complex shown in Fig. 2 , in DMSO-d_6 shows singlet signal at 2.4 ppm, corresponding to the proton of the phenolic OH [29]. The signals of the amino groups of both the anthranilic acid and the p-aminophenols appears as two adjacent signals at 6.43-6.48 ppm. The signal assigned to the proton of the carboxyl group which appears at 8.4 ppm in the spectra of the free acid [30] has been disappeared in the spectrum of the cadmium complex due to coordination of this group. The aromatic proton appears as multiplet in the region 6.63-7.8 ppm.

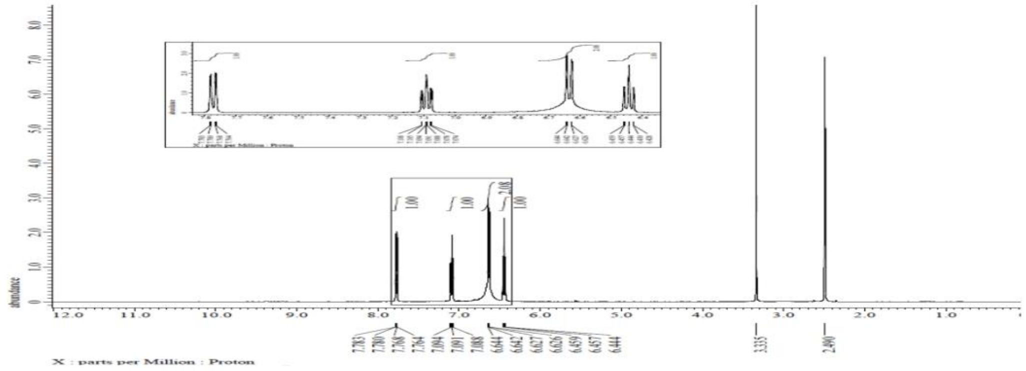

Fig. 2. 1H-NMR spectrum of Cd(II) complex.

3.3. Thermal analysis

Thermogravimetric analysis (TGA) of the Cd complex is presented in Fig 3. The measurements of the complexes were carried out in the temperature range from room temperature up to 800°C. TGA results reflects the strength of the bond and consequently the thermal stability of the complexes. The thermogrames of Cd(II) complex indicates the it decomposes in three steps tabulated in Table 2.

Table 2. TGA of Cd(II) complex.

Complex	T range (◦C)	Mass los Estim (Calcd%)	Assignment
[Cd(Anth)(p-AmPh)2]1.5H2O	25-140	1.1(1.8)	Loss of 1/2H2O
	247-350	29.3(30.8)	Loss of H2O, and C7H7NO
	351-469	42.7(44.1)	Loss of 2(C6H7NO)

The first, lies in the temperature range 25-140 ˚C due to the loss of half molecule of water of hydration (Exp., 1.1, Calcd. 1.8%). The second stage takes place in the temperature range 247-350 ˚C due to the loss of one molecule of water exists in the crystal structure but not coordinates to the metal ion [20] beside the fragment C_7H_7NO (Exp., 29.3, Calcd. 30.8%). The last step takes place in the range 351-469 ˚C, due to the loss of $2(C_6H_7N)$ (Exp. 42.7, Calcd. 44.1%). The residue attributed to CdO (Exp. 27.1, Calcd. 26.1%).

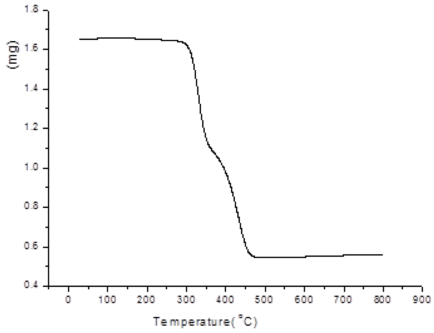

Fig. 3. TGA of Cd(II) complex.

3.4. XRD

The X-ray diffraction pattern (XRD) of the CdO synthesized by calcinations of Cd(Anthr) (p-aminophenol)2]1.5H_2O is presented in Fig. 4. The powder diffraction pattern is well indexed to CdO crystallizes in cubic system. Miller Indices (hkl) were assigned to each peak in the pattern. The pattern indicates the absence of any spurious diffractions due to crystallographic impurities. The intensity of the peaks indicates the high degree of crystallinity of the CdO.

The data showed diffraction peaks at 2θ= 33.01, 38.33, 55.31, 65.95 and 69.239 which are indexed to the planes (111), (200), (220), (311) and (222) of pure CdO nanoparticle (JCPDS 75-0592).

The crystallite size was calculated from the major diffraction peak by applying Debye-Scherrer formula $D = 0.89\ \lambda / \beta \cos\theta$ [93] Where λ is the wavelength of x-ray (1.5406 Å) for Cu K α radiation, β is full width at half maximum and θ is the peak position. The crystallite size was found to be 47 nm for the sample of CdO.

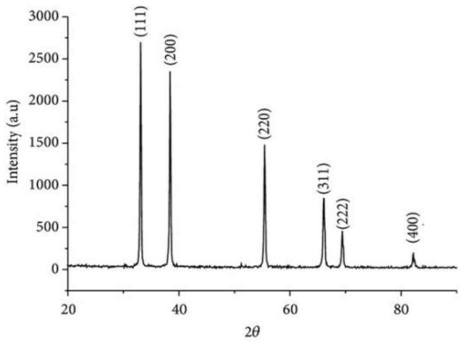

Fig. 4. X-ray diffraction pattern of CdO nanoparticles.

3.5. TEM

Fig. 5 shows the TEM images of CdO nanocromoparticles. CdO exists as nanofibers with different lengths in micrometers. The diameters of the fibers are in the range from 6-59 nm. The fibers are distributed randomly forming cross linked chains.

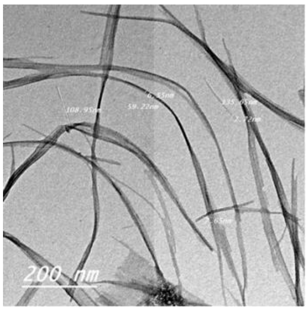

Fig. 5. TEM image of CdO nanoparticles.

3.6. Optical band gap

The conductive and semi-conductive properties of molecular materials formed from organometallic or metal-organic species give them potential use in molecular electronics. They have been used in optoelectronic devices, organic transistors and sensors [31].

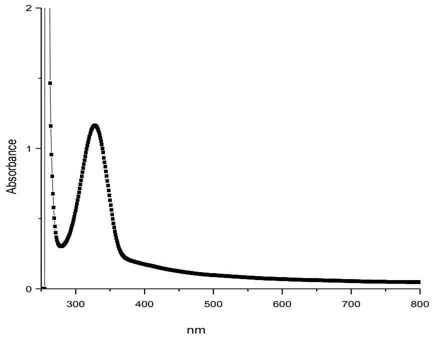

Fig. 6. Absorption spectrum of Cd(II) complex.

To clarify the conductivity of the isolated complex, the optical band gaps (E_g) of Cd(II) complex has been calculated from absorption spectra Fig. 6 .The measured absorbance (A) was used to calculate approximately the absorption coefficient (α) by using the relation:

$$\alpha = 1/d \ln A \quad (1)$$

where, d is the width of the cell.

The optical band gap (E_g) is calculated from the relation:

$$A\,h\nu = A\,(h\nu - E_g)^m \quad (2)$$

wherem is equal to 1/2 and 2 for direct and indirect transition respectively, A is an energy independent constant [32, 33]. The values of α calculated from relation (1) was used to plot $(\alpha\, h\nu)^2$ vs. hν from which a direct band gap was found Fig. 7, by extrapolating the linear portion of the curve to $(\alpha\, h\nu)^2 = 0$. From the curves, it is clear that the value of the direct band gap (E_g) of the synthesized CdO nanoparticles equal 3.9 eV is wider than the bulk (2.3 eV) due to the presence of CdO in the nano-scale. There is an indirect relation between the particle size and the optical band gap due to the electron confinement effect. The present value E_g of CdO is in the same range as some other CdO compounds synthesized by other techniques.

4. Conclusion

CdO nanoparticles were successfully synthesized and characterized by XRD and TEM techniques. The average particle sizes of CdO particles determined from XRD and TEM are about 6 nm and 59 nm. The present method is very simple, effective, and economically viable. It does not require the constraint of sophisticated equipment and pricey chemicals. Therefore, this method can be employed at large scale for the industrial production of metal oxide nanoparticles.

References

[1] C. Feldmann, H. O. Jungk, Angewandte Chemie **40**(2), 359 (2001).
[2] K. Holmberg, Handbook of Applied Surface and Colloid Chemistry, vol. 1-2, JohnWiley, New York, NY, USA, 2001.
[3] W. F. Elseviers, H. Verelst, Fuel **78**(5), 601 (1999).
[4] K. M. Abd El-Salaam, E. A. Hassan, Surface Technology **16**(2), 121 (1982).
[5] R. Mochinaga, T. Yamasaki, T. Arakawa, Sensors and Actuators B **52**(1-2), 96 (1998).
[6] D. G. Shchukin, D. V. Sviridov, A. I. Kulak, Sensors and Actuators B **76**(1–3), 556 (2001).
[7] R. S. Mane, H. M. Pathan, C. D. Lokhande, S.-H. Han, Solar Energy **80**(2), 185 (2006).
[8] D. Gal, G. Hodes, D. Lincot, H.-W. Schock, Thin Solid Films **361**, 79 (2000).
[9] R. Kaur, A. V. Singh, R. M. Mehra, Journal of Non-Crystalline Solids **352**(23-25), 2335 (2006).
[10] J. Zhang, H. Feng, W. Hao, T. Wang, Journal of Sol-Gel Science and Technology **39**(1), 37 (2006).
[11] W. Dong, C. Zhu, Optical Materials **22**, 227 (2003).
[12] D. Sarkar, S. Tikku, V. Thapar, R. S. Srinivasa, K. C. Khilar, Colloids and Surfaces A **381**(1–3), 123 (2011).
[13] M. Ristic, S. Popovic, S. Music, Materials Letters **58**, 2494 (2004).
[14] F. Zhang, F.-L. Bei, J.-M. Cao, X. Wang, Journal of Solid State Chemistry **181**(1), 143 (2008).
[15] Y. Wang, M. Li, “Materials Letters **60**, 66 (2006).
[16] R. B.Waghulade, P. P. Patil, R. Pasricha, Talanta **72**(2), 594 (2007).
[17] H. B. Lu, L. Liao, H. Li et al., Materials Letters **62**(24), 3928 (2008).
[18] N. M. Hosny, Polyhedron **30**, 470 (2011).
[19] K. Nakamoto, Infrared Spectra of Inorganic and Coordination Compounds, John Wiley, New York, 1970.
[20] S. Cakir, E. Coskun, P. Naumov, E. Bicer, J. Mol.Struct. **608**, 101 (2001).
[21] N. M. Hosny, A. Dahshan, J. Mol. Struct. **1085**, 78 (2015).
[22] N. M. Hosny, J. Mol. Struct. **923**, 98 (2009).
[23] Y. E. Sherif, N. M. Hosny, European journal of medicinal chemistry **83**, 338 (2014).
[24] N. M. Hosny, A. M. Shalaby, Transit. MetalChem. **32**, 1085 (2007).
[25] J. R. Ferraro, Low Frequency Vibrations of Inorganic and Coordination Compounds; Plenum press: New York, 1971.
[26] N. M. Hosny Journal of Coordination Chemistry **60**, 2755.
[27] N. M. Hosny, Synth. React. Inorg-Org Met Nano **6**, 391 (2010).
[28] N. M. Hosny, E. A. El Morsy, T. E. Sherif, Journal of Rare Earths **33**, 758 (2015).
[29] A. M. Hamil, K. M. Khalifa, A. AL-Houni, M. M. el-Ajaily, Rasayan J. Chem. **2**, 261 (2009).
[30] A. B. Miltojevic, N. S. Radulovic, Physics, Chemistry and Technology **13**, 121 (2015).
[31] N. F. Mott, E. A. Davis, Electrochemical Process in Non- Crystalline Materials, Calendron press, Oxford, 1979.
[32] F. Karipcin, B. Dede, Y. Caglar, D. Hur, S. Ilican, M. Caglar, Y. Sahin, Opt. Comm. **272**, 131 (2007).
[33] F. Yakuphanoglu, A. Cukurovali, I. Yilmaz, Opt. Mater. **27**, 1363 (2005).